THERMAL RESISTANCE OF A BOLTED MICROELECTRONIC CHIP CARRIER: EFFECT OF CONTACT CONDUCTANCE

C.A. Vanoverbeke[1], K.J. Negus[2], and M.M. Yovanovich[3]
Microelectronics Heat Transfer Laboratory
Department of Mechanical Engineering,University of Waterloo
Waterloo, Ontario, Canada

Abstract

An approximate expression for the thermal resistance of a bolted microelectronic chip carrier is developed by using a novel analytical approach for treating mixed boundary conditions. Results obtained for the thermal resistance indicate that there is an optimum thickness to minimize the resistance. Lift-off of the outer edge of the carrier has a negligible effect on the resistance for carriers fabricated with the optimum thickness. By increasing the amount of lift-off for carriers with a thicknesses less than the optimum value, there is often a reduction in the thermal resistance. For carriers with thicknesses above the optimum value, an increased amount of lift-off causes the resistance to rise.

Nomenclature

- a - radius of uniform heat flux source
- A_c - contact area
- A_n - series coefficient
- b - radius of device carrier
- Bi_c - Biot numbers for bottom surface of carrier
- c - inner radius of bottom surface contact area
- C_{mn} - entries in coefficient matrix
- d - outer radius of bottom surface contact area
- E - integral of errors squared
- F - applied bolt force
- G_n - entries of right hand side vector
- h_c - contact conductance for bottom surface
- $H(\cdot)$ - Heaviside step function
- $J_0(\cdot)$ - Bessel function of first kind, zero order
- $J_1(\cdot)$ - Bessel function of second kind, first order
- k - homogeneous thermal conductivity
- m - mean absolute surface slope
- N - number of series coefficients
- P - contact pressure
- q - uniform heat flux
- Q - total heat flow across top surface
- r, z - cylindrical coordinate system
- R - thermal resistance of microelectronic device carrier
- t - thickness of carrier
- T - temperature
- T_c - average temperature rise of uniform flux contact

Greek Symbols

- α - aspect ratio of carrier ($\equiv t/b$)
- γ_m - functions to evaluate C_{mn}
- δ_{mn} - Kronecker delta function ($\delta_{mn} = 0$ for $m \neq n$ $\delta_{mn} = 1$ for $m = n$)
- δ_n - eigenvalues of $J_1(\delta_n) = 0$
- ϵ_1 - relative contact size ($\epsilon \equiv a/b$)
- ϵ_2 - dimensionless inner radius of bottom surface contact ($\epsilon_2 \equiv c/b$)
- ϵ_3 - dimensionless outer radius of bottom surface contact ($\epsilon_3 \equiv d/b$)
- θ_{mn} - functions to evaluate C_{mn}
- ρ, ς - dimensionless coordinate system ($\rho = r/b$ $\varsigma = z/b$)
- ψ - dimensionless total resistance
- σ - effective RMS surface roughness
- ω_n - functions to evaluate C_{mn}

Subscripts

- c - contact between surfaces
- m, n - refers to series solution and matrix elements

Introduction

The proliferation of microelectronics throughout the aerospace and defence industries continues to grow. With many of these applications, however, increased power densities and harsh operating environments are placing tremendous demands on cooling system design. Thus thermal designers are often forced to consider cooling an individual die by using a metallic or ceramic die carrier to connect the die thermally to a large external heat sink.

The system under investigation consists of a square or hexagonal semiconductor die mounted on a cylindrical carrier which is bolted to a large heat sink as shown in Fig. 1. In the vicinity of the die and carrier, convection and radiation can be shown to be negligible modes of heat transfer relative to conduction to the heat sink. In fact a simple calculation for carriers typically less than 2 cm in diameter and 5 mm thick shows the combined convection and radiation resistance for forced-air cooling to be an order of magnitude greater that of conduction through the carrier. The thermal resistance of the carrier is of considerable interest to the thermal designer because it often represents a significant portion of the overall thermal resistance. The goal of this work is to develop an approximate analytical expresssion for the resistance of the carrier under real operating conditions.

With the conservative assumption of negligible convection and radiation, the external surfaces of the carrier are considered adiabatic. In addition the heat input from the square or hexagonal die is modelled as a uniform heat flux over a circular contact of equivalent area. Thermal resistance within the die itself could also be computed using, for example, the methods of Negus and Yovanovich[1].

[1]Undergraduate Research Assistant
[2]Graduate Research Assistant, Student Member AIAA
[3]Professor, Associate Fellow AIAA

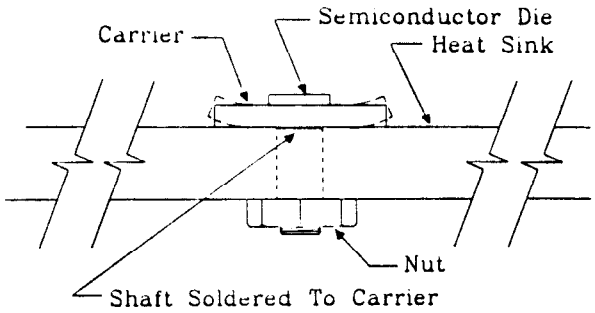

Figure 1: Typical Configuration of a Semiconductor Die Carrier Mounted to a Heat Sink

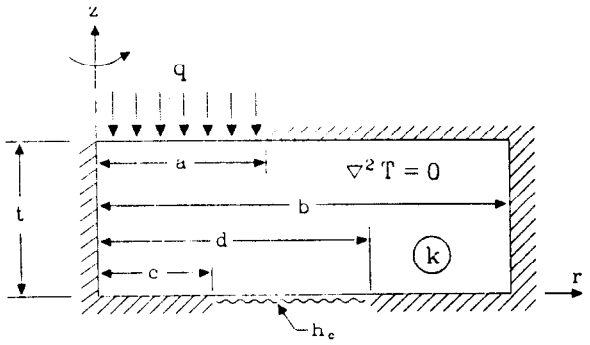

Figure 2: Basis Problem for Thermal Analysis of the Semiconductor Carrier

To attach the carrier to the heat sink, a threaded shaft is soldered to the carrier and the whole assembly is bolted to the heat sink as illustrated in Fig. 1. Thompson et al.[3] and Jofriet et al.[4] have shown that outer region of a bolted flanged connection separates when the bolt is tightened sufficently as shown by the outline in Fig. 1. The shaft connecting the carrier to the heat sink is usually made of stainless steel and the heat sink is usually made of copper or beryllia. Typical thermal conductivities for steel are 15 W/mK while copper and beryllia are approximately 400 W/mK and 270 W/mK respectively. In addition the area for heat flow in the shaft is much less than that of the heat sink. Thus the steel shaft represents a large resistance to heat flow relative to the heat sink. For a conservative estimate of the thermal resistance, the area of the carrier contacting the steel shaft is therefore considered to be insulated. These assumptions produce a basis problem as shown in Fig. 2 with a uniform flux entering a circular contact on the top surface of the carrier and a uniform contact conductance on an annular area of the bottom surface.

Many techniques are available to solve this two dimensional problem. Numerical techniques such as finite volume or finite element methods could be used to solve the problem but to perform a parametric study the computation required would be substantial. Instead the problem is solved by a novel analytic technique. Due to the combination of the adiabatic and uniform contact conductance regions on the bottom surface, this problem has a mixed boundary condition. Several techniques are available to solve mixed boundary problems but a method similar to one developed by Negus and Yovanovich[2] is incorporated in this work.

Theoretical Derivation

Under the assumptions of homogeneous isotropic thermal conductivity k and steady state conditions, heat conduction in the basis problem shown in Fig. 2 is governed by the following partial differential equation and boundary conditions:

$$\frac{1}{r}\frac{\partial}{\partial r}\left(r\frac{\partial T}{\partial r}\right) + \frac{\partial^2 T}{\partial z^2} = 0 \tag{1}$$

$$\frac{\partial T}{\partial r}(0,z) = 0 \tag{2}$$

$$\frac{\partial T}{\partial r}(b,z) = 0 \tag{3}$$

$$k\frac{\partial T}{\partial z}(r,t) = qH(a-r) \tag{4}$$

$$-k\frac{\partial T}{\partial z}(r,0) + h_c(H(r-c) - H(r-d))T(r,0) = 0 \tag{5}$$

where $H(\cdot)$ is the Heaviside unit step function and δ_n are the roots of $J_1(\delta_n) = 0$.

The solution to this problem governed by Laplace's equation with consideration of the two adiabatic boundary conditions of Eqs. (2) and (3) and the non-homogeneous boundary condition of Eq. (4) is determined in a straightforward manner using the separation of variables technique to yield

$$T(\rho,\varsigma) = \frac{qt}{k}\left\{D + \frac{\epsilon_1^2\varsigma}{\alpha} + \sum_{n=1}^{\infty}[A_n\cosh(\delta_n\varsigma) + (\omega_n - A_n\tanh(\delta_n\alpha))\sinh(\delta_n\varsigma)]J_0(\delta_n\rho)\right\} \tag{6}$$

where $\rho = r/b$ and $\varsigma = z/b$ represent dimensionless coordinates. The factor qt/k which has dimensions of temperature permits dimensionless constants D and A_n. The aspect ratio is defined as $\alpha \equiv t/b$ and the relative contact radius is defined as $\epsilon_1 \equiv a/b$ and in addition

$$\omega_n = \frac{2\epsilon_1 J_1(\delta_n\epsilon_1)}{\delta_n^2\alpha(J_0(\delta_n))^2\cosh(\delta_n\alpha)} \tag{7}$$

The classical method separation of variables technique cannot account for the mixed boundary condition of Eq. (5). An approximate analytical technique was developed by Negus and Yovanovich[2] to overcome this problem so the unknown constant D and the unknown series coefficient A_n in Eq. (6) could be evaluated from the mixed boundary condition in Eq. (5). The procedure is initiated by relating the constant D in Eq. (6) to the series coefficients A_n by substituting into Eq. (5), multiplying by $r\,dr$ and integrating from $r = 0$ to $r = b$ to give

$$D = \frac{\epsilon_1^2}{Bi_c(\epsilon_3^2 - \epsilon_2^2)} - \frac{2}{(\epsilon_3^2 - \epsilon_2^2)}\sum_{n=1}^{\infty} A_n\gamma_n \tag{8}$$

where

$$\gamma_n = \frac{\epsilon_3 J_1(\delta_n\epsilon_3) - \epsilon_2 J_1(\delta_n\epsilon_2)}{\delta_n} \tag{9}$$

and the contact Biot number for the bottom surface, the relative inner radius of the bottom contact and the relative outer radius of the bottom contact are defined respectively as

$$Bi_c \equiv \frac{h_c t}{k} \tag{10}$$

$$\epsilon_3 \equiv \frac{d}{b} \tag{11}$$

$$\epsilon_2 \equiv \frac{c}{b} \tag{12}$$

The remaining unknowns are the series coefficients A_n. Because of the mixed boundary condition on $z = 0$,

these coefficients cannot be solved directly by using the orthogonality property of the eigenfunctions (Fourier's Method). However for a finite number of coefficients N we can define

$$E=\int_0^b r\left[k\frac{\partial T}{\partial r}(r,t)+h_c[H(c-r)-H(d-r)]T(r,t)\right]^2 dr \tag{13}$$

and choose A_n such that

$$\frac{\partial E}{\partial A_m}=0 \qquad m=1,2,3,\ldots,N \tag{14}$$

where E is the continuous integral of errors squared.

A much simpler method is to apply Fourier's method to the mixed boundary condition as follows. Substituting Eqs. (8) and (6) into (5) gives

$$-\epsilon_1^2-\alpha\sum_{n=1}^{\infty}(\omega_n-A_n\tanh(\delta_n\alpha))J_0(\delta_n\varsigma)+ Bi_cD[H(r-c)-H(r-d)]+$$

$$Bi_c\sum_{n=1}^{\infty}A_n[H(r-c)-H(r-d)]J_0(\delta_n\varsigma)=0 \tag{15}$$

Multiplication of Eq. (15) by $b^2\varsigma J_0(\delta_m\varsigma)d\varsigma$ and integration from $\varsigma=0$ to $\varsigma=1$ then yields

$$-\alpha\sum_{n=1}^{\infty}[\omega_n-A_n\tanh(\delta_n\alpha)]\frac{\delta_n(J_0(\delta_n))^2}{2}\delta_{mn}+$$

$$Bi_cD\gamma_m+Bi_c\sum_{n=1}^{\infty}A_n\theta_{mn}=0 \tag{16}$$

where

$$\gamma_m=\frac{\epsilon_3J_1(\delta_m\epsilon_3)-\epsilon_2J_1(\delta_m\epsilon_2)}{\delta_m} \tag{17}$$

and for $m\neq n$

$$\theta_{mn} = \epsilon_3\left\{\frac{\delta_mJ_0(\delta_n\epsilon_3)J_1(\delta_m\epsilon_3)-\delta_nJ_0(\delta_m\epsilon_3)J_1(\delta_n\epsilon_3)}{\delta_m^2-\delta_n^2}\right\}$$

$$-\epsilon_2\left\{\frac{\delta_mJ_0(\delta_n\epsilon_2)J_1(\delta_m\epsilon_2)-\delta_nJ_0(\delta_m\epsilon_2)J_1(\delta_n\epsilon_2)}{\delta_m^2-\delta_n^2}\right\} \tag{18}$$

and for $m=n$

$$\theta_{mn} = \frac{\epsilon_3^2}{2}[(J_0(\delta_n\epsilon_3))^2+(J_1(\delta_n\epsilon_3))^2] -\frac{\epsilon_2^2}{2}[(J_0(\delta_n\epsilon_2))^2+(J_1(\delta_n\epsilon_2))^2] \tag{19}$$

Substituting Eq. (8) into Eq. (16) and isolating the unknown series coefficients results in an infinite system of linear algebraic equations of the form

$$[C_{mn}]\{A_n\}=\{G_m\} \tag{20}$$

where

$$C_{mn} = \frac{\delta_n\alpha\tanh(\delta_n\alpha)(J_0(\delta_n))^2\delta_{mn}}{2} -\frac{2Bi_c\gamma_m\gamma_n}{\epsilon_3^2-\epsilon_2^2}+Bi_c\theta_{mn} \tag{21}$$

$$G_m = \frac{\omega_m\delta_m\alpha(J_0(\delta_m))^2}{2}-\frac{\gamma_m\epsilon^2}{\epsilon_3^2-\epsilon_2^2} \tag{22}$$

An approximate solution for the temperature distribution is obtained by solving a finite subset of the infinite system of linear equations of Eq. (20). Any desired degree of accuracy can be achieved, in theory, by increasing the number of series coefficients.

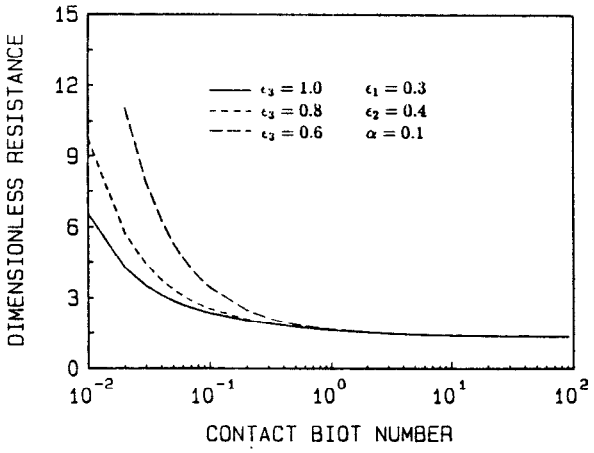

Figure 3: Dimensionless Thermal Resistance: Effect of Decreasing Bottom Surface Contact Area

One interesting point to note is the limiting case where ϵ_2 approaches zero and ϵ_3 approaches one. In this case the mixed boundary condition goes to a homogeneous Robin boundary condition along the bottom surface. It can be easily shown that the off diagonal entries are all zero and that the series coefficients are identical to the coefficients obtained by applying Fourier's method for this limiting case.

The thermal resistance of the carrier is given by the definition

$$R=\frac{\bar{T}_c-T_\infty}{Q} \tag{23}$$

where for this problem $T_\infty=0$ and Q is the total heat flow rate crossing the top surface of the carrier or

$$Q=q\pi a^2 \tag{24}$$

The average temperature rise on the contact portion on the top surface of the carrier is defined as

$$\bar{T}_c=\frac{1}{\pi a^2}\int_0^a 2\pi rT(r,t)dr \tag{25}$$

A dimensionless thermal resistance is defined as

$$\psi=4kaR \tag{26}$$

Using the approximate solution of Eq. (6) and combining it with Eqs. (23–26), an approximate expression for the dimensionless thermal resistance is given

$$\psi \approx \frac{4\alpha\epsilon_1}{\pi}+\frac{4D\alpha}{\pi\epsilon_1}+\frac{8\alpha}{\pi\epsilon_1^3}\sum_{n=1}^{N}[A_n\mathrm{sech}(\delta_n\alpha) -\Omega_n\tanh(\delta_n\alpha)]\frac{\epsilon_1J_1(\delta_n\epsilon_1)}{\delta_n} \tag{27}$$

where

$$\Omega_n=\frac{2\epsilon_1J_1(\delta_n\epsilon_1)}{\alpha\delta_n^2(J_0(\delta_n))^2} \tag{28}$$

with N coefficients A_n determined by solving Eq. (20).

Implementation and Results of the Solution

To evaluate the dimensionless resistance given by Eq. (27), the solution of Eq. (20) for a finite number of series coefficients A_n is required. The formulation of the system of equations is accomplished by substituting for C_{mn} and G_n from Eqs. (21) and (22). A Cholesky decomposition solver with optimized pivoting was used to solve for the unknown series coefficents A_n. The solver and expression for the resistance were programmed in Microsoft Fortran on an IBM-PC. As many as 250 coefficients could be determined within the 640K byte memory limitation of this microcomputer.

The dimensionless thermal resistance is a function five of dimensionless parameters or

$$\psi = \psi(Bi_c, \alpha, \epsilon_1, \epsilon_2, \epsilon_3) \tag{29}$$

By using the five dimensionless parameters in Eq. (29), the number of independent parameters is reduced from the original seven (a, b, c, d, t, h_c, t) to five. Even with this reduction in the number of independent parameters a comprehensive parametric study is difficult to achieve.

To demonstrate the major influences of some of the various dimensionless parameters, dimensionless resistances were evaluated for a wide range of values. The parameter ϵ_2 was fixed at the value of 0.4 while the value of ϵ_3 was decreased to show the effect of a smaller contact area (or larger "lift-off") on the bottom surface. In order to keep the number of plots to mininum, the value of ϵ_1 was fixed at 0.3. The three remaining paramenters were varied and the results are plotted in Figs. 3 and 4.

Several important effects are observed for the variations in the parameters, Bi_c, ϵ_2 and α in Figs. 3 and 4. First, the dimensionless resistance approaches a constant value for large values of the Biot number as expected since the bottom contact approaches an isothermal condition for sufficiently large Bi_c. As the aspect ratio of carrier is increased the resistance often increases because the heat has to flow through more material. However, from Figs. 3 and 4, it is obvious that this phenomena does not occur for all Biot numbers. The simple explanation is that in these cases the increased aspect ratio decreases the constriction resistance and this has a larger effect than the increase of the material resistance. When the value of the Biot number is small there is an increase in the overall resistance because the contact resistance becomes larger relative to the material resistance. From Fig. 3, it is also apparent that for a small aspect ratio the overall resistance becomes independent of the contact area for large Biot numbers. When the aspect ratio is small, heat cannot easily conduct radially along the carrier and thus spread uniformily across the carrier-heat sink interface. With little heat spreading over the contact, the outer region of the contact has little effect on the resistance of the carrier as evident from the computed results.

A Practical Example

A specific example problem is given to show the practical implementation of the solution developed. In this example problem a die with a equivalent radius of 4 mm is placed on die carrier with an overall radius of 12 mm. A stud 4 mm in diameter is silver soldered to the bottom surface of the die carrier. The size of the die is not a parameter the thermal designer has much control over therefore its value will remain constant during the analysis. The size of the die carrier is limited by the overall chip packing density and consequently is taken to be fixed also. Since a specified stud size is normally incorporated, the size of the stud remains fixed in this analysis of the die carrier.

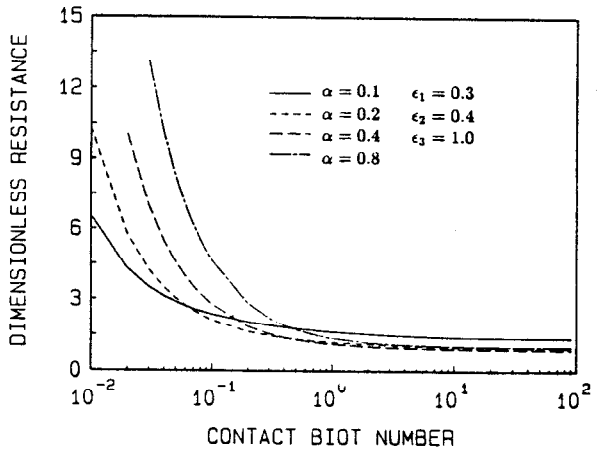

Figure 4: Dimensionless Thermal Resistance: Effect of Increasing Thickness

Material	Conductivity (W/mK)	Hardness (MPa)
Copper	400	803
Aluminum	237	1470
Aluminum Oxide	36	23226
Beryllium Oxide	272	11172
Kovar	16	2185

Table 1: Properties of Materials Used for Die Carrier Construction

With the values of a,c and b fixed, the remaining parameters that can be varied are t,d,k, and h_c. The conductivity k is determined by the type of material used for the construction of the die carrier. The range of thicknesses was chosen to vary from 1 - 10 mm. The remaining two parameters d and h_c are a function of the torque applied in tightening the nut. As more torque is applied to the nut a larger downward force is applied to the bottom surface of the die carrier. By increasing this force the thermal resistance of the die carrier will vary according to the effects of increased contact conductance and lower contact area.

To predict the contact conductance a correlation developed by Yovanovich[7] is used and is given by

$$h_c = \frac{1.25km}{\sigma}\left(\frac{P}{H}\right)^{0.95} \tag{30}$$

where σ is the effective RMS surface roughness, m the mean absolute surface slope, P the contact pressure and H the hardness of the material. The contact pressure is a function of the applied load and is obtained from

$$P = \frac{F}{A_c} \tag{31}$$

where F is the applied bolt load and $A_c = \pi(d^2 - c^2)$ is the contact area on the bottom surface. From Eqs. (30) and (31), it is obvious that the contact conductance is not only a function of the applied load but it is also a function of the contact area. However, the contact area is dependent on the applied load because the outer edge of the chip carrier begins to lift-off as the bolt load is increased.

As mentioned previously, Jofriet et al[4]. investigated the separation of a flanged connection when the bolt is sufficiently tightened. In their work the flange separation was caused by the bolt head and nut faces pushing inward on two flange plates. For the chip carrier, however, the separation from the heat sink is due to the stud pulling down on the central area soldered to the stud and prediction of the actual region is more difficult.

Since the contact area can not be evaluated easily for this situation, the value of d or the contact area is varied independent of the load applied to at least determine its importance to the overall thermal resistance. To simplify the analysis, a fixed load is chosen while contact area is being varied.

The analysis of the chip carrier in this example problem was performed for different materials to investigate the effect of surface hardness and thermal conductivity. Typical materials available for the construction of the chip carrier are copper, Kovar, aluminum oxide and beryllium oxide and the properties of these materials are summarized in Table 1. The hardness in Eq. (30) is for the softer material and since the heat sink is assumed to be made of aluminum its properties are also shown in Table 1. From Table 1, it is obvious that hardness of aluminum is used except for a copper carrier. Two important parameters for the evaluation of the contact conductance are the surface roughness and mean surface slope. Since these parameters depend on the individual surfaces from which information is not available, typical values of $\sigma = 2\mu$m and $m = 0.1$ were chosen for all of the surfaces. The maximum bolt force is limited by the tensile strength of the solder used to join and stud and chip carrier. A solder with 97.5% lead and 2.5% silver with a tensile strength of about $30MPa$ was assumed to be used. A bolt force of $F = 200\ N$ was chosen as it is well below the failure force of about 1500 N for a 4 mm diameter stud. Values for the outside radius of the bottom contact area were chosen to be 6, 9, and 12 mm respectively.

The thermal resistance of the carrier versus thickness is plotted in Figs. 5–8 for the different materials and the values d of discussed previously. For all of the materials, there is an optimum thickness which gives the minimum resistance of the carrier for a given contact area. Note that there is little difference in the optimum thicknesses and minimum resistances for the different contact areas or different amounts of lift-off being considered. Thus with a carrier designed to optimum thickness, the thermal designer does not have to be concerned with the effect of lift-off.

An interesting point is that for thicknesses less than the optimum value the resistance is actually lower for increased lift-off. When the carrier is thin, lift-off is desireable feature which is easily attained because is not very stiff. The thermal benefit occurs because there are two competing effects which greatly influence the overall resistance for thin carriers. The first effect is the resistance to heat flow due to contact resistance on the bottom surface. The second effect represents the potentially large resistance to heat transfer in the radial direction when a thin carrier behaves as a one dimensional fin. The contact

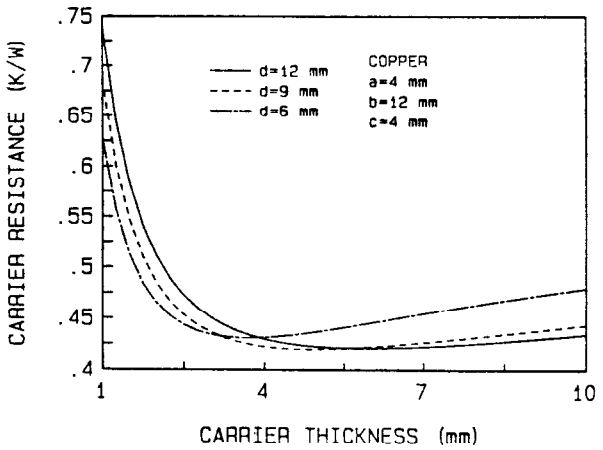

Figure 5: Thermal Resistance of a Copper Die Carrier for Various Thickenesses and Contact Areas

resistance is often approximated by the one dimensional form $R_c \approx 1/h_c A_c$. For given h_c, the contact resistance should increase as A_c decreases. However, in this case where the total load is fixed, a smaller contact area has increased contact pressure which causes the contact conductance to rise. The net effect of increasing contact conductance and decreasing area has little effect on the contact resistance. However, by increasing the amount of lift-off, the effective conduction length in the radial direction is decreased and therefore the overall resistance decreases for sufficiently thin carriers.

At thicknesses above the optimum value, the overall resistance increases with increasing thickness but the increase is small for the working range of thicknesses being investigated. Also, the effect of lift-off becomes more predominant as the thickness is increased. Even though the effects of lift-off become important to the resistance, it still might be negligible because the thicker carriers are much stiffer and do not readily lift-off.

A final consideration is the effect of the type of material chosen for the construction of the carrier. For copper the maximum resistance is computed as $0.75K/W$ while for Kovar it is $21K/W$. The maximum resistance for aluminum oxide is $9.5K/W$ and for beryllium oxide it is $1.25K/W$. Thus from a thermal standpoint, copper is the obvious material to choose. Unfortunately copper has a much different thermal expansion coefficient than that of the silicon die and this can lead to fatigue failure due to stress problems. Also, if the die is to be electrically isolated, copper is eliminated. Ironically, Kovar is the optimum choice to relieve expansion problems but it is the worst for a thermal design. Aluminum oxide and beryllium oxide have similar expansion coefficients to silicon which are not as good as Kovar but are much better than copper. Aluminum oxide has a much smaller thermal conductivity than beryllium oxide and thus beryllium oxide is an excellent choice for high power applications.

Summary and Conclusions

In this work an approximate model to predict the thermal resistance of a semiconductor die carrier has been developed by considering a fundamental basis problem for heat conduction in the carrier. An approximate analytical solution for the basis problem was derived by using a technique for handling the mixed boundary condition.

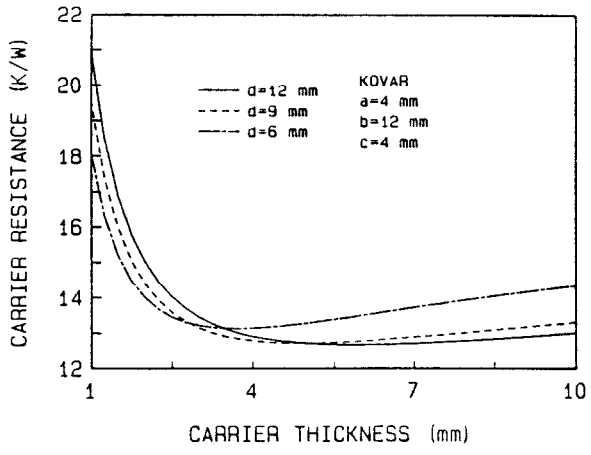

Figure 6: Thermal Resistance of Kovar Die Carrier for Various Thickenesses and Contact Areas

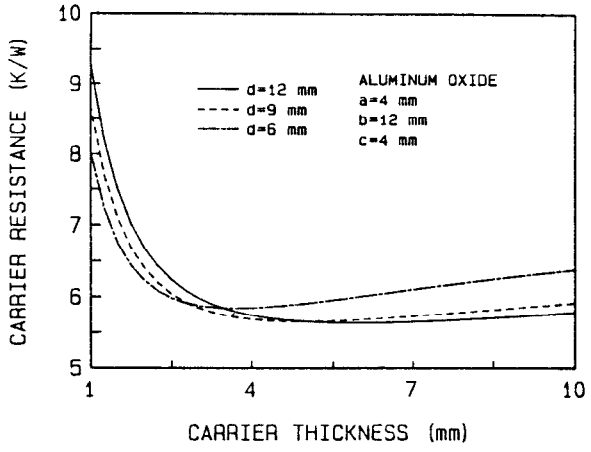

Figure 7: Thermal Resistance of the Aluminum Oxide Die Carrier for Various Thickenesses and Contact Areas

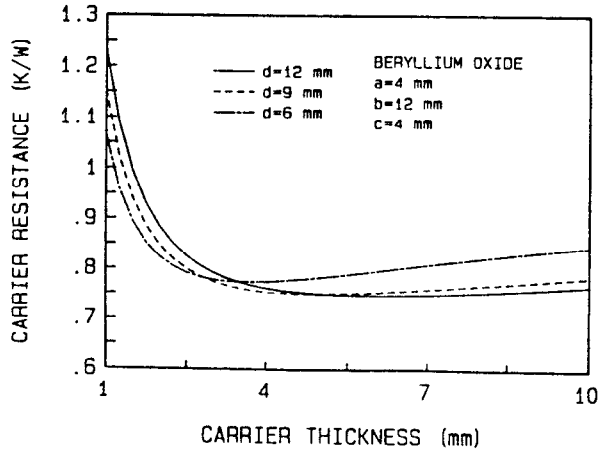

Figure 8: Thermal Resistance of the Beryllium Oxide Die Carrier for Various Thickenesses and Contact Areas

The solution allows the thermal designer to choose optimal geometric and loading criteria for obtaining the lowest possible thermal reistance.

There is range of optimum thicknesses for different amounts of lift-off which give the minimum reistance of the carrier. The minimum resistance for a carrier designed with the optimum thickness is not a strong function of the amount of lift-off of the carrier. Carriers with a thickness much less than the optimum value often have a lower resistance for increased amounts of lift-off. A thickness well above the optimum value does not usually increase the overall resistance substantially.

Acknowledgements

The authors acknowledge the financial support of the Natural Sciences and Engineering Research Council under operating grant A7455 for Dr. Yovanovich and from a Postgraduate Scholarship for Mr. Negus.

References

1. Negus, K.J. and Yovanovich, M.M., 1987, "Thermal Computations in a Semiconductor Die Using Surface Elements and Infinite Images", International Symposium on Cooling Technology in Electronic Equipment, Honolulu, HA, Mar. 18-21.
2. Negus, K.J. and Yovanovich, M.M., 1986, "Thermal Analysis and Optimization of Convectively Cooled Microelectronic Circuit Boards",*Heat Transfer In Electronic Equipment*, ASME HTD-Vol. 57, pp. 167-176.
3. Thompson, J.C.,Sze, V., Strevel, D.G., and Jofriet, J.C.,1976, "The Interface Boundary Conditions for Bolted Flanged Connections", ASME Paper No. 76-PVP-4, ASME Petroleum Mechanical Engineering and Pressure Vessels and Piping Conference, Mexico City, Mexico, Sept. 19–24.
4. Jofriet,J.C., Sze, Y., and Thompson, J.C., 1981, "Further Studies for the Interface Boundary Conditions for Bolted Flanged Connections", *ASME Journal of Pressure Vessel Technology*, Vol. 103, pp. 240-245.
5. Abramowitz, M. and Stegun, I., 1965, *Handbook of Mathematical Functions*, Dover, New York.
6. Spiegel, M.R., 1968, *Mathematical Handbook of Formulas and Tables*, McGraw-Hill, New York.
7. Yovanovich, M.M., 1982, "Thermal Contact Correlations", *Spacecraft Radiative Transfer and Temperature Control*, Vol. 83 of Progress in Astronautics and Aeronautics, ed. Horton, T.E., AIAA, New York, pp. 83-95.
8. American Society for Metals, 1979, *Metals Handbook Ninth Edition Volume 2 Properties and Selections:Nonferrous Alloys and Pure Metals*, American Society for Metals, Metals Park, Ohio.